## Altermagnetic Shastry-Sutherland fullerene networks

Jiaqi Wu, <sup>1,\*</sup> Alaric Sanders, <sup>2,\*</sup> Rundong Yuan, <sup>2</sup> and Bo Peng<sup>2,†</sup>

<sup>1</sup>Peterhouse, University of Cambridge, Trumpington Street, Cambridge CB2 1RD, UK

<sup>2</sup>Theory of Condensed Matter Group, Cavendish Laboratory,
University of Cambridge, J. J. Thomson Avenue, Cambridge CB3 0HE, UK

(Dated: September 15, 2025)

The interplay between quantum magnetism and many-body physics is of fundamental importance in condensed matter physics. Molecular building blocks provide a versatile platform for exploring the exotic quantum phases arising from complex orderings in frustrated lattices. Here we demonstrate a showcase system based on altermagnetic Shastry-Sutherland fullerene networks, which can be constructed from a  $C_{40}$  molecular synthon with two effective spin-1/2 sites due to the resonance structures. The charge-neutral, pure-carbon systems exhibit an altermagnetic ground state with fully compensated spins arranged in alternating  $C_{40}$  units in a 2D rutile-like lattice, leading to d-wave splitting of the spin-polarised electronic band structure and strong chiral-split magnons. We report a rich phase diagram including altermagentic, quantum spin liquid, plaquette, and dimer phases, which can be accessed via moderate strains. Our findings open a new avenue for exploring quantum many-body physics based on scalable, chemically-feasible, molecular quantum materials.

Magnetism in low-dimensional systems provides fertile ground for the discovery of exotic quantum phases  $^{1-5}$ . Beyond conventional ferromagnetism and antiferromagnetism, altermagnetism has emerged as a newlyidentified class of collinear magnetism with compensated spin sublattices but finite momentum-dependent spin polarisation <sup>6-14</sup>. The vanishing net magnetisation and symmetry-protected spin splitting offer tantalising opportunities for next-generation quantum devices with robust spin-polarised transport. Moreover, the interplay between altermagnetism and many-body physics leads to a rich variety of quantum phenomena such as superconductivity <sup>15,16</sup>, spin liquid <sup>17</sup>, Hubbard model <sup>18–21</sup>, and Kondo lattice <sup>22</sup>. In this context, quantum magnets in the Shastry-Sutherland model <sup>23–29</sup> represent a showcase model to realise altermagnetism, as their neighbouring sublattices are connected by rotations and glide reflections in the absence of neither translational nor inversion symmetry <sup>30</sup>. Furthermore, the Shastry-Sutherland lattice provides an ideal platform to explore the exotic quantum physics and complex many-body effects in altermagnets such as superconductivity <sup>31,32</sup>, strong correlation <sup>33</sup>, quantum phase transition <sup>34,35</sup>, and spin frustrations <sup>36,37</sup>. Yet, realising altermagnetism in the Shastry-Sutherland lattice remains a challenge.

Carbon-based materials provide unpaired  $\pi$  electrons in delocalised  $p_z$  orbitals, which are typically found in defects such as edges, vacancies, or heteroatom sites that disrupt homogeneous electron density  $^{38-40}$ . However, it is challenging to synthesise these systems due to atomically-precise, periodic assembly of the defected carbon fragments into the  $\pi$ -conjugated frameworks. Comparing to carbon fragments, fullerene building blocks are promising alternatives due to their stable units and

highly-tuneable structures. We have recently discovered approaches to systematically introduce magnetism into pure-carbon, charge neutral, fullerene monolayers by enforcing crystalline symmetry based on molecularorbital theory 41 or by creating  $\pi$  magnetism from resonating valence bond <sup>42</sup>, opening new avenues for realising exotic quantum phases such as quantum anomalous Hall effects in otherwise non-magnetic monolayers <sup>43</sup>. Most importantly, the inherent ability of assembling these molecules into periodic frameworks has been confirmed since the synthesis of polymeric C<sub>60</sub> monolayers 44, as demonstrated by their rich structural phases as predicted theoretically  $^{45-53}$  and synthesised experimentally <sup>54–56</sup>. Therefore, it would be insightful to introduce altermagnetism into fullerene-based networks as a promising platform to realise exotic models such as the Shastry-Sutherland lattice.

Here, we use fullerene building blocks to design quantum altermagnets in 2D Shastry-Sutherland lattice. The key to the realisation of altermagnetism lies in the elegant design of a molecular network that incorporates both a  $C_{40}$  unit, with unpaired electrons for  $\pi$  magnetism, and a rutile-like 2D lattice, for constructing two sublattices with opposite spins. We show that the resonance structure of the C<sub>40</sub> cage provides six carbon sites for two unpaired electrons on the opposite sides of the molecule and stabilises two effective spin-1/2 sites, which, upon assembly into a rutile-like monolayer, realise an altermagnetic ground state. Our first-principles calculations reveal dwave splitting in the electronic bands and strong chiralsplit magnon dispersions. Most remarkably, the altermagnetic Shastry-Sutherland networks can be continuously tuned into the frustrated quantum spin liquid phase through moderate strain. Our work opens a new frontier that unites the chemistry of carbon-based molecules with the physics of strongly-frustrated quantum magnetism.

Altermagnetic fullerene networks. Figure 1a shows a  $C_{40}$  fullerene molecular synthon, which serves as a

<sup>\*</sup> These authors contributed equally.

<sup>†</sup> bp432@cam.ac.uk

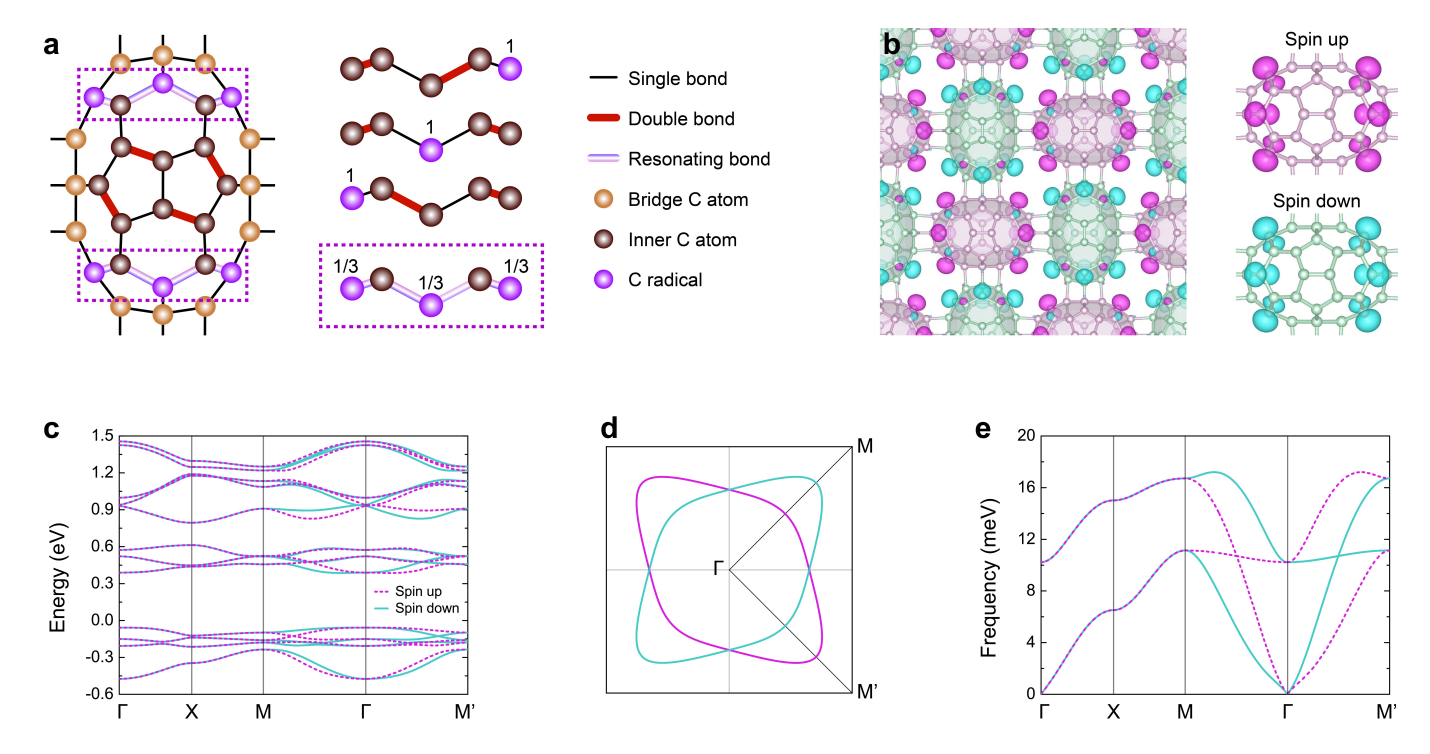


FIG. 1. Altermagnetism in monolayer  $C_{40}$  fullerene networks. a  $C_{40}$  building block and its resonance structures, b spin densities, c band structures, d iso-energy surface at  $0.025 \,\mathrm{eV}$  below the VBM for d-wave order, and e chiral-split magnons.

stable building block that has been synthesised decades  $ago^{57-59}$ . Among the thirty carbon atoms on the top surface of  $C_{40}$ , there are twelve fully-saturated carbon atoms with  $sp^3$  hybridisation for intermolecular bonds (marked in yellow). For the eight carbon atoms from the two five-membered rings in the centre of  $C_{40}$ , each atom is surrounded by three single bonds due to the  $sp^2$  hybridisation, leaving eight  $p_z$  electrons to form four double bonds as marked by red in Fig. 1a. Consequently, all twenty carbon atoms above are non-magnetic.

We then focus on the ten carbon atoms in two W-shaped chains, as highlighted in purple boxes in Fig. 1a. For each W-shaped cluster, there are three pairing schemes for two double bonds between the five carbon atoms, leaving one unpaired electron at the leftmost, middle and rightmost sites of the chain, respectively. The resonance structure leads to an averaged distribution of  $1/3~\mu_{\rm B}$  magnetic moment per purple carbon atom and a quantised total magnetic moment of 1  $\mu_{\rm B}$  for the group of five atoms in the W-shaped chain. Therefore, a C<sub>40</sub> unit has six magnetic carbon atoms with a total magnetic moment of 2  $\mu_{\rm B}$ , as confirmed by first-principles calculations.

Afterwards, we construct closely-packed fullerene networks by rotating neighbouring  $C_{40}$  building units by  $\pi/2$ , and such  $C_4$  rotation creates a 2D rutile-like lattice similar to  $\mathrm{RuO_2}^{13}$ . The space-efficient arrangement of fullerene molecules is expected to stabilise the structure as found experimentally  $^{44,54}$ . Most interestingly, the closely-packed lattice leads to an altermagnetic ground state that is energetically favourable than the ferromag-

netic, non-magnetic and other antiferromagnetic order, respectively. This suggests stronger intramolecular exchange interactions than the intermolecular coupling (as discussed later). Figure 1b shows the corresponding spin densities where magenta (cyan) iso-surface represents spin-up (spin-down) states. Within each  $C_{40}$  unit, the evenly distributed spin densities among the six magnetic carbon atoms confirm the resonance structure of 1/3  $\mu_{\rm B}$ per magnetic carbon atom. The neighbouring  $C_{40}$  units are connected by  $C_4$  rotations and  $G_x/G_y$  glide reflections in the absence of neither translational nor inversion symmetry, leading to compensated antiparallel magnetic order. Such an alternating order of the magnetic moments results in a zero net magnetisation. Additionally, for fullerene units with light carbon elements, the spin-orbit coupling approaches the non-relativistic limit. Therefore, the vanishing net magnetisation has a strong non-relativistic origin.

We next examine the band structures of altermagnetic  $C_{40}$  networks in Fig.1c. The spin-up and spin-down bands are doubly degenerate along the  $\Gamma$ -X-M high-symmetry paths. Along M- $\Gamma$ -M', however, the symmetry-protected collinear compensated magnetic order in real space generates an alternating spin polarisation in the band structure in the reciprocal momentum space, and the spin-up and spin-down bands become split, breaking the time-reversal symmetry without magnetisation. We further compute the iso-energy surface at 0.025 eV below the valence band maximum (VBM), which corresponds to moderate hole doping. As shown in Fig.1d, the spin orientations at time-reversed, opposite

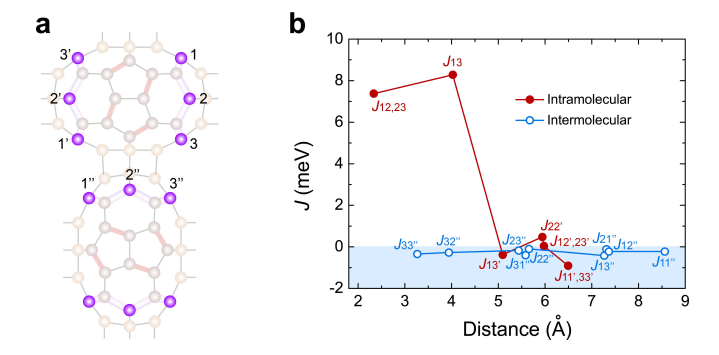


FIG. 2. Exchange interactions in altermagnetic  $C_{40}$  monolayers. a Magnetic carbon atoms and b their corresponding exchange interactions as a function of distance.

momenta on the iso-energy surface are the same (non-time-reversed), while the spin-up and spin-down bands are symmetric, exhibiting typical features for d-wave order similar to  $\mathrm{RuO_2}^{13}$ .

To further confirm the altermagnetism, we compute the magnon dispersion. As shown in Fig. 1e, the lowfrequency magnons near  $\Gamma$  show linear dispersion, which is a typical antiferromagnetic/altermagnetic feature<sup>60</sup>. The degenerate magnon bands along  $\Gamma$ -X-M exhibit giant chiral splitting along M-Γ-M' in the absence of spinorbit coupling. The chiral magnon modes have either left-handed or right-handed spin precession along a given Néel vector with opposite precessional angular momentum. Similar to the spin splitting in the electronic band structure, the chiral splitting of magnon bands in altermagnets even without relativistic effects differs altermagnets from ferromagnets and antiferromagnets 61,62, giving rise to novel applications in altermagnetic spintronics and magnonics. All magnon frequencies are real and non-negative with a global minimum at  $\Gamma$ , which, again, indicates a stable altermagnetic ground state <sup>63</sup>.

Exchange interactions. We then examine the exchange interactions in altermagnetic  $C_{40}$  monolayers. As shown in Fig. 2a, the three magnetic carbon atoms in the W-shaped chain share one  $\pi$  electron, forming an effective spin-1/2 group. The exchange interactions between atoms i and j within one effective spin-1/2 group are denoted as  $J_{ij}$ , the intramolecular interactions between the two effective spin-1/2 groups are denoted as  $J_{ij'}$ , while the intermolecular interactions from the nearest neighbouring effective spin-1/2 groups are denoted as  $J_{ij''}$ .

Figure 2b summarises the calculated J parameters as a function of distance between these magnetic atoms. Within one effective spin-1/2 group, the interactions are ferromagnetic, with much stronger coupling strength  $(J_{ij} > 7 \, \text{meV})$  than  $J_{ij'}$  and  $J_{ij''}$ .

Intramolecular  $J_{ij'}$  coupling is much smaller (between -0.9 and 0.5 meV) than  $J_{ij}$ . The antiferromagnetic couplings ( $J_{13'}=-0.38$  meV,  $J_{11'}=J_{33'}=-0.90$  meV) are stronger than the ferromagnetic ones ( $J_{22'}=0.48$  meV,  $J_{12'}=J_{23'}=0.04$  meV). Interestingly, the long-range

exchange interactions  $J_{11'}$  and  $J_{33'}$  from the largest intramolecular distance of 6.49 Å have the strongest coupling strength, whilst the smallest  $J_{12'}$  and  $J_{23'}$  have a relatively shorter distance of 5.98 Å.

The intermolecular interactions are all antiferromagnetic, with much weaker interaction strength than that of the intramolecular coupling. The largest intermolecular coupling comes from atom 1 and atom 3"  $(J_{13''}=-0.42\,\mathrm{meV})$  at a distance of 7.27 Å, whereas the smallest intermolecular coupling corresponds to  $J_{22''}=-0.10\,\mathrm{meV}$  at a smaller distance of 5.65 Å. The intermolecular interactions beyond the nearest neighbouring group quickly decay to zero.

## Phase diagram of the Shastry-Sutherland lattice. Having understood the exchange interactions of monolayer $C_{40}$ networks, we can build a lattice spin model by treating the three magnetic atoms in the effective spin-1/2 group as one spin-1/2 site, as these three atoms have dominant ferromagnetic interactions.

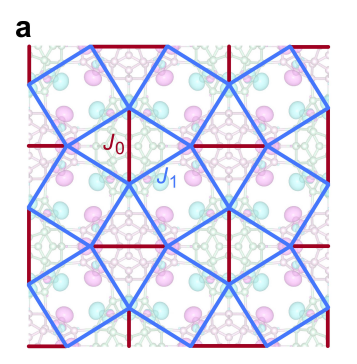
The effective spin-1/2 sites form the well-known Shastry-Sutherland lattice, as shown in Fig. 3a. The effective exchange interactions between these effective spin-1/2 sites can be divided into two groups – intramolecular exchange  $J_0$  (marked in dark red) and intermolecular exchange  $J_1$  (marked in blue). The effective exchange interactions can be defined as

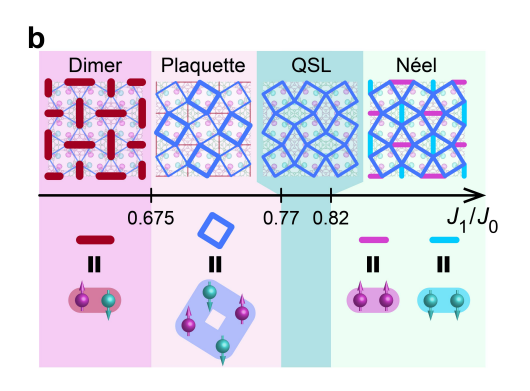
$$J_{\text{eff}} = \frac{\sum S_i^{(1)} J_{ij}^{(1,2)} S_j^{(2)}}{\sum S_i^{(1)} \sum S_j^{(2)}},$$
 (1)

where  $S_i^{(1)}$  and  $S_j^{(2)}$  indicate electron spin (taken as 1/6) from atomic site i from effective spin-1/2 group 1 and atomic site j from effective group 2 respectively, and  $J_{ij}^{(1,2)}$  represents their exchange interactions. The intramolecular  $J_0$  can be computed by choosing two effective spin-1/2 groups within the same molecule (i.e.,  $J_{ij'}$  in Fig. 2a), while the  $J_1$  can be calculated from the intermolecular, nearest neighbouring effective spin-1/2 groups (i.e.,  $J_{ij'}$  in Fig. 2a).

For monolayer  $C_{40}$  networks, we obtain effective exchange interactions  $J_0 = -0.21\,\mathrm{meV}$  and  $J_1 = -0.25\,\mathrm{meV}$ , leading to a ratio  $J_1/J_0$  of 1.18. According to the phase diagram for the Shastry-Sutherland lattice in Fig. 3 b, this corresponds to the Néel phase where  $J_1$  dominates over  $J_0$ , and the Shastry-Sutherland lattice effectively reduces to the altermagnetic ground state as we find in *ab initio* calculations. In the Néel state, the two spins within one  $C_{40}$  unit are the same, whereas neighbouring fullerene molecules have opposite spins, which is exactly the ground-state altermagnetic phase.

The phase diagram can be tuned by the ratio between intermolecular and intramolecular coupling  $J_1/J_0$ . As shown in Fig. 3 b, decreasing the  $J_1/J_0$  ratio to 0.82 leads to a quantum spin liquid phase due to the frustrations between the intramolecular and intermolecular exchange couplings. This exotic phase has promising applications such as error-resistant topological qubits <sup>64</sup>. When the





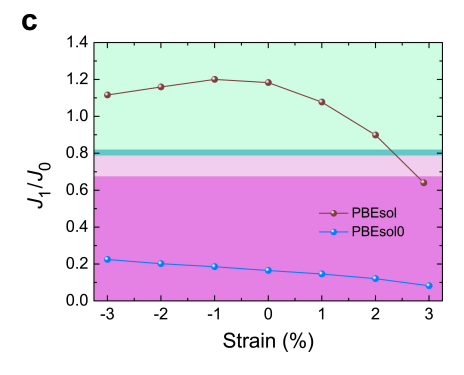


FIG. 3. Phase diagram of Shastry-Sutherland  $C_{40}$  fullerene networks. a Shastry-Sutherland lattice, b phase diagram, and c order parameter  $J_1/J_0$  as a function of bi-axial strain computed from semi-local PBEsol and hybrid-functional PBEsol0.

 $J_1/J_0$  ratio lies between 0.77 and 0.675, a phase of independent "plaquette" units is formed, where each unit consists of four spins. This is known as the plaquette phase. In 2D C<sub>40</sub> networks, this phase corresponds to four spins located on four molecules around an interstice. Further decreasing the  $J_1/J_0$  ratio below 0.675 results in the dimer valence bond solid phase. In the dimer phase, the two spins on each fullerene pair up into a singlet state as the intramolecular  $J_0$  dominates, and the neighbouring singlet pairs stop to interact with each other.

To tune the ratios between  $J_1$  and  $J_0$ , we introduce biaxial strains. Figure 3 **c** shows the  $J_1/J_0$  ratios computed for monolayer C<sub>40</sub> networks under varied strain. For biaxial strains between -3 and 2%, the systems remain in the Néel order, indicating an altermagnetic ground state. When further increasing the strains to 3%, the  $C_{40}$  system passes through both the quantum spin liquid and plaquette phases, until reaching the dimer region. We use a strain step of 0.1% between 2-3% strains. In the quantum spin liquid region,  $J_1$  and  $J_0$  become illdefined, and our first-principles calculations show strong frustrations in the computed exchange interactions. In the plaquette phase, the four calculated  $J_1$  terms around one spin-1/2 site are no longer symmetry equivalent but exhibit strong anisotropy, which agrees with the phase behaviours. Upon reaching the dimer phase, the four  $J_1$ terms around one spin-1/2 site are equal again, leading to a well defined  $J_1/J_0$  ratio.

Further unscreened hybrid functional calculations suggest that the dimer phase is stable at all strains between  $\pm 3\%$  in the zero-screening limit, which provides the lower bound for  $J_1/J_0$  in free-standing monolayers without any substrates. This suggests that the phase transitions can be induced through control of screening effects such as the application of substrates with varied dielectric constants. Additionally, the dimer phase itself also exhibits rich physics such as triplon-bound state and spin-nematic ordering  $^{65-68}$ , which can be further tuned by chemical decoration and exohedral doping. This will unlock future opportunities in realising room-temperature, organic quantum altermagnets to explore the complex many-body effects.

Methods. Density functional theory (DFT) calculations <sup>69,70</sup> are performed using the Vienna ab initio Simulation Package (VASP) 71,72 under the generalised gradient approximation (GGA) formalism with projector augmented wave (PAW) basis sets <sup>73,74</sup>. The Perdew-Burke-Ernzerhof functional corrected for solids (PBEsol) <sup>75</sup> is used along with C  $2s^22p^2$  as valence electrons. A planewave cutoff of 800 eV is employed and the self-consistent field energy convergence criterion is set to be  $10^{-6}$  eV. The Brillouin zone is sampled with a converged k-mesh of  $3 \times 3$ . Spin polarisation is included throughout all the calculations. The crystal structures are fully relaxed using the conjugate gradient method <sup>76</sup> until the Hellmann-Feynman forces are less than  $10^{-2} \,\mathrm{eV/Å}$ . The vacuum spacing between monolayers is set to be more than 20 Å, and dipole corrections are employed perpendicular to the monolayers to eliminate interactions between periodic images <sup>77</sup>. A Wannier tight-binding model <sup>78–80</sup> is constructed using Wannier90 81-83 by projecting Wannier functions onto each  $\sigma$  bond centre, with  $sp^2$  carbon atoms having an extra Wannier function to mimic the  $p_z$  orbitals. This bond-centre approach has been widely used in fullerene molecules <sup>81</sup> and leads to 188 Wannier functions in a unit cell of two  $C_{40}$  molecules. The exchange interactions are computed from the Green's function method <sup>84,85</sup> using the TB2J package <sup>86</sup> where the positions of Wannier centres and the magnetic moments are carefully checked. The magnon dispersion is computed under the Holstein-Primakoff transformation 87 based on the bosonic Hamiltonian 88, as implemented in the MAGNOPY package that has been widely used to study low-dimensional antiferromagnets <sup>89,90</sup>. The chirality of magnons with band index j is defined as the right-handed (RH) or left-handed (LH) spin precession along a given Néel vector with opposite precessional angular momentum <sup>61,91</sup>. To analyse the effect of strain, the lattice parameters are modified (with respect to the fully relaxed structure) and fixed, while the atomic coordinates are allowed to fully relax. Unscreened hybrid functional PBEsol0 calculations 92 are also performed to study the exchange interactions in the zero-screening limit.

**Acknowledgment.** We thank Samzi Tishler at the University of Cambridge for proof reading. J.W. acknowledges support from the Cambridge Undergraduate Research Opportunities Programme and from Peterhouse for the James Porter Scholarship. B.P. acknowledges support from Magdalene College Cambridge for a Nevile Research Fellowship. The calculations were performed using resources provided by the Cambridge Service for Data Driven Discovery (CSD3) operated by the University of Cambridge Research Computing Service (www.

csd3.cam.ac.uk), provided by Dell EMC and Intel using Tier-2 funding from the Engineering and Physical Sciences Research Council (capital grant EP/T022159/1), and DiRAC funding from the Science and Technology Facilities Council (http://www.dirac.ac.uk), as well as with computational support from the UK Materials and Molecular Modelling Hub, which is partially funded by EPSRC (EP/T022213/1, EP/W032260/1 and EP/P020194/1), for which access was obtained via the UKCP consortium and funded by EPSRC grant ref EP/P022561/1.

<sup>1</sup> Kewei Sun, Nan Cao, Orlando J. Silveira, Adolfo O. Fumega, Fiona Hanindita, Shingo Ito, Jose L. Lado, Peter Liljeroth, Adam S. Foster, and Shigeki Kawai, "Onsurface synthesis of heisenberg spin-1/2 antiferromagnetic molecular chains," Science Advances 11, eads1641 (2025).

 $^{2}\,$  Xuelei Su, Zhihao Ding, Ye Hong, Nan Ke, Ka<br/>King Yan, Can Li, Yi-Fan Jiang, and Ping Yu, "Fabrication of spin-1/2 heisenberg antiferromagnetic chains via combined onsurface synthesis and reduction for spinon detection," Nature Synthesis 4, 694-701 (2025).

 $^3$  Xiaoshuai Fu, Li<br/> Huang, Kun Liu, João C. G. Henriques, Yixuan Gao, Xianghe Han, Hui Chen, Yan Wang, Carlos-Andres Palma, Zhihai Cheng, Xiao Lin, Shixuan Du, Ji Ma, Joaquín Fernández-Rossier, Xinliang Feng, and Hong-Jun Gao, "Building spin-1/2 antiferromagnetic heisenberg chains with diaza-nanographenes," Nature Synthesis 4, 684-693 (2025).

Xinnan Peng and Jiong Lu, "Spin-1/2 heisenberg chains realized in  $\pi$ -electron systems," Nature Synthesis 4, 668– 670 (2025).

- Shaotang Song, Yu Teng, Weichen Tang, Zhen Xu, Yuanyuan He, Jiawei Ruan, Takahiro Kojima, Wenping Hu, Franz J. Giessibl, Hiroshi Sakaguchi, Steven G. Louie, and Jiong Lu, "Janus graphene nanoribbons with localized states on a single zigzag edge," Nature 637, 580-586 (2025).
- Satoru Hayami, Yuki Yanagi, and Hiroaki Kusunose, "Momentum-dependent spin splitting by collinear antiferromagnetic ordering," J. Phys. Soc. Jpn. 88, 123702 (2019).
- Lin-Ding Yuan, Zhi Wang, Jun-Wei Luo, Emmanuel I. Rashba, and Alex Zunger, "Giant momentum-dependent spin splitting in centrosymmetric low-z antiferromagnets," Phys. Rev. B **102**, 014422 (2020).
- Libor Šmejkal, Rafael González-Hernández, T. Jungwirth, and J. Sinova, "Crystal time-reversal symmetry breaking and spontaneous hall effect in collinear antiferromagnets," Science Advances 6, eaaz8809 (2020).
- Hai-Yang Ma, Mengli Hu, Nana Li, Jianpeng Liu, Wang Yao, Jin-Feng Jia, and Junwei Liu, "Multifunctional antiferromagnetic materials with giant piezomagnetism and noncollinear spin current," Nature Communications 12, 2846 (2021).
- Igor I. Mazin, Klaus Koepernik, Michelle D. Johannes, Rafael González-Hernández, and Libor Šmejkal, "Prediction of unconventional magnetism in doped FeSb<sub>2</sub>," Proc Natl Acad Sci 118, e2108924118 (2021).
- <sup>11</sup> Libor Šmejkal, Jairo Sinova, and Tomas Jungwirth,

"Emerging research landscape of altermagnetism," Phys. Rev. X 12, 040501 (2022).

<sup>12</sup> Libor Šmejkal, Jairo Sinova, and Tomas Jungwirth, "Beyond conventional ferromagnetism and antiferromagnetism: A phase with nonrelativistic spin and crystal rotation symmetry," Phys. Rev. X 12, 031042 (2022).

- <sup>13</sup> Olena Fedchenko, Jan Minár, Akashdeep Akashdeep, Sunil Wilfred D'souza, Dmitry Vasilyev, Olena Tkach, Lukas Odenbreit, Quynh Nguyen, Dmytro Kutnyakhov, Nils Wind, Lukas Wenthaus, Markus Scholz, Kai Rossnagel, Moritz Hoesch, Martin Aeschlimann, Benjamin Stadtmüller, Mathias Kläui, Gerd Schönhense, Tomas Jungwirth, Anna Birk Hellenes, Gerhard Jakob, Libor Šmejkal, Jairo Sinova, and Hans-Joachim Elmers, "Observation of time-reversal symmetry breaking in the band structure of altermagnetic RuO<sub>2</sub>," Science Advances 10, eadj4883 (2024).
- J. Krempaský, L. Šmejkal, S. W. D'Souza, M. Hajlaoui, G. Springholz, K. UhlíVision Res.ová, F. Alarab, P. C. Constantinou, V. Strocov, D. Usanov, W. R. Pudelko, R. González-Hernández, A. Birk Hellenes, Z. Jansa, H. Reichlová, Z. Šobáň, R. D. Gonzalez Betancourt, P. Wadley, J. Sinova, D. Kriegner, J. Minár, J. H. Dil, and T. Jungwirth, "Altermagnetic lifting of kramers spin degeneracy," Nature **626**, 517–522 (2024).
- Anjishnu Bose, Samuel Vadnais, and Arun Paramekanti, "Altermagnetism and superconductivity in a multiorbital  $t - i \mod 2$ , Phys. Rev. B **110**, 205120 (2024).
- <sup>16</sup> Lucas V. Pupim and Mathias S. Scheurer, "Adatom engineering magnetic order in superconductors: Applications to altermagnetic superconductivity," Phys. Rev. Lett. 134, 146001 (2025).
- João Augusto Sobral, Subrata Mandal, and Mathias S. Scheurer, "Fractionalized altermagnets: From neighboring and altermagnetic spin liquids to spin-symmetric band splitting," Phys. Rev. Res. 7, 023152 (2025).
- Toshihiro Sato, Sonia Haddad, Ion Cosma Fulga, Fakher F. and Jeroen van den Brink, "Altermagnetic anomalous hall effect emerging from electronic correlations," Phys. Rev. Lett. 133, 086503 (2024).
- Purnendu Das, Valentin Leeb, Johannes Knolle, Michael Knap, "Realizing altermagnetism in fermihubbard models with ultracold atoms," Phys. Rev. Lett. **132**, 263402 (2024).
- Samuele Giuli, Carlos Mejuto-Zaera, and Massimo Capone, "Altermagnetism from interaction-driven itinerant magnetism," Phys. Rev. B 111, L020401 (2025).
- Saisai He, Jize Zhao, Hong-Gang Luo, and Shijie Hu,

"Altermagnetism and beyond in the  $t-t'-\delta$  fermi-hubbard model," Phys. Rev. B **112**, 035108 (2025).

<sup>22</sup> Miaomiao Zhao, Wei-Wei Yang, Xueming Guo, Hong-Gang Luo, and Yin Zhong, "Altermagnetism in heavy-fermion systems: Mean-field study on the kondo lattice," Phys. Rev. B 111, 085145 (2025).

<sup>23</sup> B. Sriram Shastry and Bill Sutherland, "Exact ground state of a quantum mechanical antiferromagnet," Physica B+C 108, 1069–1070 (1981).

<sup>24</sup> Shin Miyahara and Kazuo Ueda, "Exact dimer ground state of the two dimensional heisenberg spin system srcu<sub>2</sub>(bo<sub>3</sub>)<sub>2</sub>," Phys. Rev. Lett. **82**, 3701–3704 (1999).

Christian Knetter, Alexander Bühler, Erwin Müller-Hartmann, and Götz S. Uhrig, "Dispersion and symmetry of bound states in the shastry-sutherland model," Phys. Rev. Lett. 85, 3958–3961 (2000).

Akihisa Koga and Norio Kawakami, "Quantum phase transitions in the shastry-sutherland model for srcu<sub>2</sub>(bo<sub>3</sub>)<sub>2</sub>," Phys. Rev. Lett. 84, 4461–4464 (2000).

Andreas Läuchli, Stefan Wessel, and Manfred Sigrist, "Phase diagram of the quadrumerized shastry-sutherland model," Phys. Rev. B 66, 014401 (2002).

<sup>28</sup> J. Dorier, K. P. Schmidt, and F. Mila, "Theory of magnetization plateaux in the shastry-sutherland model," Phys. Rev. Lett. **101**, 250402 (2008).

<sup>29</sup> A. Brassington, Q. Ma, G. Sala, A. I. Kolesnikov, K. M. Taddei, Y. Wu, E. S. Choi, H. Wang, W. Xie, J. Ma, H. D. Zhou, and A. A. Aczel, "Magnetic properties of the quasi-xy shastry-sutherland magnet er<sub>2</sub>be<sub>2</sub>sio<sub>7</sub>," Phys. Rev. Mater. 8, 094001 (2024).

Francesco Ferrari and Roser Valentí, "Altermagnetism on the shastry-sutherland lattice," Phys. Rev. B 110, 205140 (2024).

Ohung-Hou Chung and Yong Baek Kim, "Competing orders and superconductivity in the doped mott insulator on the shastry-sutherland lattice," Phys. Rev. Lett. 93, 207004 (2004).

Bohm-Jung Yang, Yong Baek Kim, Jaejun Yu, and Kwon Park, "Doped valence-bond solid and superconductivity on the shastry-sutherland lattice," Phys. Rev. B 77, 104507 (2008).

Jun Liu, Nandini Trivedi, Yongbin Lee, B. N. Harmon, and Jörg Schmalian, "Quantum phases in a doped mott insulator on the shastry-sutherland lattice," Phys. Rev. Lett. 99, 227003 (2007).

<sup>34</sup> Jong Yeon Lee, Yi-Zhuang You, Subir Sachdev, and Ashvin Vishwanath, "Signatures of a deconfined phase transition on the shastry-sutherland lattice: Applications to quantum critical srcu<sub>2</sub>(bo<sub>3</sub>)<sub>2</sub>," Phys. Rev. X 9, 041037 (2019).

Zhenzhong Shi, Sachith Dissanayake, Philippe Corboz, William Steinhardt, David Graf, D. M. Silevitch, Hanna A. Dabkowska, T. F. Rosenbaum, Frédéric Mila, and Sara Haravifard, "Discovery of quantum phases in the shastry-sutherland compound srcu2(bo3)2 under extreme conditions of field and pressure," Nature Communications 13, 2301 (2022).

<sup>36</sup> M. Pula, S. Sharma, J. Gautreau, Sajilesh K. P., A. Kanigel, M. D. Frontzek, T. N. Dolling, L. Clark, S. Dunsiger, A. Ghara, and G. M. Luke, "Candidate for a quantum spin liquid ground state in the shastry-sutherland lattice material yb<sub>2</sub>be<sub>2</sub>geo<sub>7</sub>," Phys. Rev. B **110**, 014412 (2024).

<sup>37</sup> Philippe Corboz, Yining Zhang, Boris Ponsioen, and

Frédéric Mila, "Quantum spin liquid phase in the shastry-sutherland model revealed by high-precision infinite projected entangled-pair states," arXiv:2502.14091 (2025).

Oleg V Yazyev, "Emergence of magnetism in graphene materials and nanostructures," Rep. Prog. Phys. 73, 056501 (2010).

Michael Slota, Ashok Keerthi, William K. Myers, Evgeny Tretyakov, Martin Baumgarten, Arzhang Ardavan, Hatef Sadeghi, Colin J. Lambert, Akimitsu Narita, Klaus Müllen, and Lapo Bogani, "Magnetic edge states and coherent manipulation of graphene nanoribbons," Nature 557, 691–695 (2018).

<sup>40</sup> Ruize Ma, Nikita V. Tepliakov, Arash A. Mostofi, and Michele Pizzochero, "Electrically tunable ultraflat bands and π-electron magnetism in graphene nanoribbons," J. Phys. Chem. Lett. 16, 1680–1685 (2025).

<sup>41</sup> Jiaqi Wu, Leonard Werner Pingen, and Bo Peng, "Symmetry-induced magnetism in fullerene monolayers," arXiv:2508.18125 (2025).

<sup>42</sup> Bo Peng and Michele Pizzochero, "Designing antiferromagnetic spin-1/2 chains in janus fullerene nanoribbons," arXiv:2508.18849 (2025).

<sup>43</sup> Leonard Werner Pingen, Jiaqi Wu, and Bo Peng, "Tunable quantum anomalous hall effect in fullerene monolayers," arXiv:2508.19849 (2025).

<sup>44</sup> Lingxiang Hou, Xueping Cui, Bo Guan, Shaozhi Wang, Ruian Li, Yunqi Liu, Daoben Zhu, and Jian Zheng, "Synthesis of a monolayer fullerene network," Nature 606, 507–510 (2022).

<sup>45</sup> Bo Peng, "Monolayer fullerene networks as photocatalysts for overall water splitting," J. Am. Chem. Soc. **144**, 19921– 19931 (2022).

<sup>46</sup> Bo Peng, "Stability and Strength of Monolayer Polymeric C<sub>60</sub>," Nano Lett. **23**, 652–658 (2023).

<sup>47</sup> Cory Jones and Bo Peng, "Boosting photocatalytic water splitting of polymeric c60 by reduced dimensionality from two-dimensional monolayer to one-dimensional chain," J. Phys. Chem. Lett. 14, 11768–11773 (2023).

<sup>48</sup> Jiaqi Wu and Bo Peng, "Smallest [5,6]fullerene as building blocks for 2d networks with superior stability and enhanced photocatalytic performance," J. Am. Chem. Soc. 147, 1749–1757 (2025).

<sup>49</sup> Dylan Shearsby, Jiaqi Wu, Dekun Yang, and Bo Peng, "Tuning electronic and optical properties of 2d polymeric c60 by stacking two layers," Nanoscale 17, 2616–2620 (2025).

Darius Kayley and Bo Peng, "C<sub>60</sub> building blocks with tuneable structures for tailored functionalities," Computational Materials Today 6, 100030 (2025).

Armaan Shaikh and Bo Peng, "Negative and positive anisotropic thermal expansion in 2d fullerene networks," arXiv: , 2504.02037 (2025).

<sup>52</sup> Bo Peng and Michele Pizzochero, "Electronic structure of fullerene nanoribbons," ACS Nano 19, 29637–29645 (2025).

<sup>53</sup> Bo Peng and Michele Pizzochero, "Monolayer C<sub>60</sub> networks: a first-principles perspective," Chem. Commun. **61**, 10287–10302 (2025).

Elena Meirzadeh, Austin M. Evans, Mehdi Rezaee, Milena Milich, Connor J. Dionne, Thomas P. Darlington, Si Tong Bao, Amymarie K. Bartholomew, Taketo Handa, Daniel J. Rizzo, Ren A. Wiscons, Mahniz Reza, Amirali Zangiabadi, Natalie Fardian-Melamed, Andrew C. Crowther, P. James Schuck, D. N. Basov, Xiaoyang Zhu, Ashutosh Giri,

- Patrick E. Hopkins, Philip Kim, Michael L. Steigerwald, Jingjing Yang, Colin Nuckolls, and Xavier Roy, "A few-layer covalent network of fullerenes," Nature **613**, 71–76 (2023).
- Taotao Wang, Li Zhang, Jinbao Wu, Muqing Chen, Shangfeng Yang, Yalin Lu, and Pingwu Du, "Few-layer fullerene network for photocatalytic pure water splitting into h<sub>2</sub> and h<sub>2</sub>o<sub>2</sub>," Angew. Chem. Int. Ed. **62**, e202311352 (2023).
- Yuxuan Zhang, Yifan Xie, Hao Mei, Hui Yu, Minjuan Li, Zexiang He, Wentao Fan, Panpan Zhang, Antonio Gaetano Ricciardulli, Paolo Samorì, Mengmeng Li, and Sheng Yang, "Electrochemical synthesis of 2d polymeric fullerene for broadband photodetection," Adv. Mater. 37, 2416741 (2025).
- <sup>57</sup> F. N. Tomilin, P. V. Avramov, S. A. Varganov, A. A. Kuzubov, and S. G. Ovchinnikov, "Possible scheme of synthesis-assembling of fullerenes," Physics of the Solid State 43, 973–981 (2001).
- <sup>58</sup> Andrey N. Enyashin and Alexander L. Ivanovskii, "Structural, electronic, cohesive, and elastic properties of diamondlike allotropes of crystalline C<sub>40</sub>," Phys. Rev. B 77, 113402 (2008).
- <sup>59</sup> Alexey Kharlamov, Ganna Kharlamova, Marina Bondarenko, and Veniamin Fomenko, "Joint Synthesis of Small Carbon Molecules (C<sub>3</sub>-C<sub>11</sub>), Quasi-Fullerenes (C<sub>40</sub>, C<sub>48</sub>, C<sub>52</sub>) and their Hydrides," Chemical Engineering and Science 1, 32–40 (2013).
- 60 Charles Kittel, <u>Introduction to solid state physics</u> (Wiley New York, 1976).
- <sup>61</sup> Libor Šmejkal, Alberto Marmodoro, Kyo-Hoon Ahn, Rafael González-Hernández, Ilja Turek, Sergiy Mankovsky, Hubert Ebert, Sunil W. D'Souza, Ondřej Šipr, Jairo Sinova, and Tomáš Jungwirth, "Chiral Magnons in Altermagnetic RuO<sub>2</sub>," Phys. Rev. Lett. **131**, 256703 (2023).
- <sup>62</sup> Yi-Fan Zhang, Xiao-Sheng Ni, Ke Chen, and Kun Cao, "Chiral magnon splitting in altermagnetic crsb from first principles," Phys. Rev. B 111, 174451 (2025).
- Andres Tellez-Mora, Xu He, Eric Bousquet, Ludger Wirtz, and Aldo H. Romero, "Systematic determination of a material's magnetic ground state from first principles," npj Computational Materials 10, 20 (2024).
- <sup>64</sup> Kai Klocke, Yue Liu, Gábor B Halász, and Jason Alicea, "Spin-liquid-based topological qubits," arXiv:2411.08093 (2024).
- M. E. Zayed, Ch. Rüegg, J. Larrea J., A. M. Läuchli, C. Panagopoulos, S. S. Saxena, M. Ellerby, D. F. Mc-Morrow, Th. Strässle, S. Klotz, G. Hamel, R. A. Sadykov, V. Pomjakushin, M. Boehm, M. Jiménez-Ruiz, A. Schneidewind, E. Pomjakushina, M. Stingaciu, K. Conder, and H. M. Ronnow, "4-spin plaquette singlet state in the shastry-sutherland compound srcu2(bo3)2," Nature Physics 13, 962–966 (2017).
- <sup>66</sup> P. A. McClarty, F. Krüger, T. Guidi, S. F. Parker, K. Refson, A. W. Parker, D. Prabhakaran, and R. Coldea, "Topological triplon modes and bound states in a Shastry-Sutherland magnet," Nature Physics 13, 736–741 (2017).
- <sup>67</sup> Zhentao Wang and Cristian D. Batista, "Dynamics and instabilities of the shastry-sutherland model," Phys. Rev. Lett. **120**, 247201 (2018).
- <sup>68</sup> Dirk Wulferding, Youngsu Choi, Seungyeol Lee, Mikhail A. Prosnikov, Yann Gallais, Peter Lemmens, Chengchao Zhong, Hiroshi Kageyama, and Kwang-Yong Choi, "Thermally populated versus field-induced triplon bound states

- in the shastry-sutherland lattice  $srcu_2(bo_3)_2$ ," npj Quantum Materials 6, 102 (2021).
- <sup>69</sup> P. Hohenberg and W. Kohn, "Inhomogeneous electron gas," Phys. Rev. **136**, B864–B871 (1964).
- W. Kohn and L. J. Sham, "Self-consistent equations including exchange and correlation effects," Phys. Rev. 140, A1133–A1138 (1965).
- <sup>71</sup> G. Kresse and J. Furthmüller, "Efficient iterative schemes for ab initio total-energy calculations using a plane-wave basis set," Phys. Rev. B **54**, 11169–11186 (1996).
- <sup>72</sup> G. Kresse and J. Furthmüller, "Efficiency of ab-initio total energy calculations for metals and semiconductors using a plane-wave basis set," Computational Materials Science 6, 15 – 50 (1996).
- <sup>73</sup> P. E. Blöchl, "Projector augmented-wave method," Phys. Rev. B **50**, 17953–17979 (1994).
- <sup>74</sup> G. Kresse and D. Joubert, "From ultrasoft pseudopotentials to the projector augmented-wave method," Phys. Rev. B **59**, 1758–1775 (1999).
- John P. Perdew, Adrienn Ruzsinszky, Gábor I. Csonka, Oleg A. Vydrov, Gustavo E. Scuseria, Lucian A. Constantin, Xiaolan Zhou, and Kieron Burke, "Restoring the Density-Gradient Expansion for Exchange in Solids and Surfaces," Phys. Rev. Lett. 100, 136406 (2008).
- M. C. Payne, M. P. Teter, D. C. Allan, T. A. Arias, and J. D. Joannopoulos, "Iterative minimization techniques for ab initio total-energy calculations: molecular dynamics and conjugate gradients," Rev. Mod. Phys. 64, 1045–1097 (1992).
- <sup>77</sup> G. Makov and M. C. Payne, "Periodic boundary conditions in ab initio calculations," Phys. Rev. B **51**, 4014–4022 (1995).
- Nicola Marzari and David Vanderbilt, "Maximally localized generalized Wannier functions for composite energy bands," Phys. Rev. B 56, 12847–12865 (1997).
- <sup>79</sup> Ivo Souza, Nicola Marzari, and David Vanderbilt, "Maximally localized Wannier functions for entangled energy bands," Phys. Rev. B 65, 035109 (2001).
- Nicola Marzari, Arash A. Mostofi, Jonathan R. Yates, Ivo Souza, and David Vanderbilt, "Maximally localized Wannier functions: Theory and applications," Rev. Mod. Phys. 84, 1419–1475 (2012).
- Arash A. Mostofi, Jonathan R. Yates, Young-Su Lee, Ivo Souza, David Vanderbilt, and Nicola Marzari, "Wannier90: A tool for obtaining maximally-localised Wannier functions," Computer Physics Communications 178, 685–699 (2008).
- Arash A. Mostofi, Jonathan R. Yates, Giovanni Pizzi, Young-Su Lee, Ivo Souza, David Vanderbilt, and Nicola Marzari, "An updated version of Wannier90: A tool for obtaining maximally-localised Wannier functions," Computer Physics Communications 185, 2309–2310 (2014).
- 83 Giovanni Pizzi, Valerio Vitale, Ryotaro Arita, Stefan Blügel, Frank Freimuth, Guillaume Géranton, Marco Gibertini, Dominik Gresch, Charles Johnson, Takashi Koretsune, Julen Ibañez-Azpiroz, Hyungjun Lee, Jae-Mo Lihm, Daniel Marchand, Antimo Marrazzo, Yuriy Mokrousov, Jamal I Mustafa, Yoshiro Nohara, Yusuke Nomura, Lorenzo Paulatto, Samuel Poncé, Thomas Ponweiser, Junfeng Qiao, Florian Thöle, Stepan S Tsirkin, Malgorzata Wierzbowska, Nicola Marzari, David Vanderbilt, Ivo Souza, Arash A Mostofi, and Jonathan R Yates, "Wannier90 as a community code: new features and applications," J. Phys.: Condens. Matter 32, 165902 (2020).

- <sup>84</sup> A.I. Liechtenstein, M.I. Katsnelson, V.P. Antropov, and V.A. Gubanov, "Local spin density functional approach to the theory of exchange interactions in ferromagnetic metals and alloys," Journal of Magnetism and Magnetic Materials 67, 65–74 (1987).
- <sup>85</sup> Dm. M. Korotin, V. V. Mazurenko, V. I. Anisimov, and S. V. Streltsov, "Calculation of exchange constants of the heisenberg model in plane-wave-based methods using the green's function approach," Phys. Rev. B 91, 224405 (2015).
- <sup>86</sup> Xu He, Nicole Helbig, Matthieu J. Verstraete, and Eric Bousquet, "Tb2j: A python package for computing magnetic interaction parameters," Computer Physics Communications 264, 107938 (2021).
- <sup>87</sup> T. Holstein and H. Primakoff, "Field dependence of the intrinsic domain magnetization of a ferromagnet," Phys. Rev. 58, 1098–1113 (1940).
- <sup>88</sup> J.H.P. Colpa, "Diagonalization of the quadratic boson

- hamiltonian," Physica A: Statistical Mechanics and its Applications **93**, 327–353 (1978).
- Andrey Rybakov, Carla Boix-Constant, Diego Alba Venero, Herre S. J. van der Zant, Samuel Mañas-Valero, and Eugenio Coronado, "Probing short-range correlations in the van der waals magnet crsbr by small-angle neutron scattering," Small Sci. 4, 2400244– (2024).
- Ocarla Boix-Constant, Andrey Rybakov, Clara Miranda-Pérez, Gabriel Martínez-Carracedo, Jaime Ferrer, Samuel Mañas-Valero, and Eugenio Coronado, "Programmable magnetic hysteresis in orthogonally-twisted 2d crsbr magnets via stacking engineering." Adv. Mater. 37, 2415774—(2025).
- <sup>91</sup> Rundong Yuan, Wojciech J Jankowski, Ka Shen, and Robert-Jan Slager, "Quantum geometry of altermagnetic magnons probed by light," arXiv:2508.02781 (2025).
- Oarlo Adamo and Vincenzo Barone, "Toward reliable density functional methods without adjustable parameters: The pbe0 model," J. Chem. Phys. 110, 6158–6170 (1999).